Pricing Options with Green's Functions when Volatility, Interest Rate, and Barriers Depend on Time

Dorfleitner, Gregor; Schneider, Paul; Hawlitschek, Kurt; Buch, Arne

QUANTITATIVE FINANCE

Pricing Options with Green's Functions when Volatility, Interest Rate, and Barriers Depend on Time

Journal:	*Quantitative Finance*
Manuscript ID:	RQUF-2005-0087.R1
Manuscript Category:	Research Paper
Date Submitted by the Author:	06-Jun-2006
Complete List of Authors:	Dorfleitner, Gregor; Institute for Finance and Financial Markets, Finance & Accounting Schneider, Paul Hawlitschek, Kurt Buch, Arne
Keywords:	Numerical Methods for Option Pricing., Partial Differential Equations, Derivatives Pricing, Barrier Options, Green's function
JEL Code:	G13 - Contingent Pricing|Futures Pricing < G1 - General Financial Markets < G - Financial Economics

Note: The following files were submitted by the author for peer review, but cannot be converted to PDF. You must view these files (e.g. movies) online.

GFOP_final.tex
master1.bib

Pricing Options with Green's Functions when Volatility, Interest Rate and Barriers Depend on Time

Gregor Dorfleitner*, Paul Schneider*, Kurt Hawlitschek†, Arne Buch*

Abstract

We derive the Green's function for the Black/Scholes partial differential equation with time-varying coefficients and time-dependent boundary conditions. We provide a thorough discussion of its implementation within a pricing algorithm that also accommodates American style options. Greeks can be computed as derivatives of the Green's function. Generic handling of arbitrary time-dependent boundary conditions suggests our approach to be used with the pricing of (American) barrier options, although options without barriers can be priced equally well. Numerical results indicate that knowledge of the structure of the Green's function together with the well developed tools of numerical integration make our approach fast and numerically stable.

Keywords: Green's Function, time-dependent coefficients, numerical methods, option pricing, (double) barrier options, American options

*Institute of Finance and Financial Markets, Vienna University of Economics and Business Administration
†Mendelstraße 8, 89081 Ulm, Germany

1 Introduction

Arbitrage-free prices of financial securities driven by diffusion processes satisfy the fundamental pricing partial differential equation. This applies to derivatives written on traded assets, but also carries over to instruments that are subject to relative pricing such as fixed-income derivatives. In its most general form the coefficients of the fundamental pricing PDE are time- and state-dependent. As a special case the coefficients of the Black/Scholes (B/S) PDE are neither time nor state-dependent. In this paper we treat the case of time-dependent coefficients. Closed-form solutions are not available in general for this PDE. Instead it can be solved numerically. In practice this is usually accomplished by finite differencing, special cases thereof such as binomial or trinomial lattice techniques, and Monte Carlo simulation. We refer the reader to recent discussions in (Andricopoulos, Widdicks, Duck, and Newton, 2003, Section I) and (Staunton, 2005).

Green's functions are specifically related to PDE's with a special type of boundary value problem.[1] Once the Green's function is found for a PDE, it can be solved by integration. Green's functions have mainly been used in the finance literature for standard end condition problems without boundary conditions, i.e. options with arbitrary payoffs in a classical B/S environment.[2] Further applications of Green's functions include callable bonds as in Beaglehole and Tenney (1992) and Büttler and Waldvogel (1996). Mallier and Deakin (2003) consider the same for convertible bonds. The Green's function approach presented below provides a solution to the Black and Scholes PDE generalized to *time-varying coefficients*. It gives a general pricing formula for options with arbitrary payoffs and up to two arbitrary boundary conditions, which makes our framework particularly applicable to the pricing of single and double barrier options and American barrier options. As long as the barriers happen to follow a specific form determined by the time-variable coefficients, the approach leads to a closed-form solution. For any other case we propose a new numerical algorithm which is easily implemented and yields pricing precision comparable to finite differencing, while maintaining the amenities that come with the knowledge of the Green's function such as computation of the Greeks by simply taking partial derivatives of the Green's function with respect to the underlying variables. In our paper we term this procedure the *stripe method*.

For single and double barrier options in the classical B/S framework several analytic formulae are

[1] John (1986)

[2] (see e.g. Duffie, 2001; Wilmott, 2000). In this paper we distinguish between "end conditions" (payoffs) and "boundary conditions" (barriers) (see Figure 1 for an illustration).

known. The formula collections in Haug (1997) or Zhang (2001) provide an extensive coverage of what is available. In these surveys single and double barrier options are priced for the case of constant barriers, constant coefficients and constant rebates. The paper of Kunitomo and Ikeda (1992) provides a pricing formula for double barrier options with two curved barriers (of a specific form). Hui, Lo, and Yuen (2000) show how this formula can also be derived with Green's functions. We generalize their approach to time-dependent coefficients and also time-dependent rebates when barriers are touched. Roberts and Shortland (1997) or Lo, Lee, and Hui (2003) also consider the case of time-dependent coefficients, but restrict themselves to single barrier options. Furthermore, they are only concerned with finding upper and lower bounds for the option value. Option pricing with time-dependent parameters (but no barriers) is also treated by Wilmott (2000, p. 131ff). When barriers are involved the matter is much less obvious and Wilmott's approach cannot be applied. To the best of our knowledge our formula is the first closed-form solution for up to two barriers in the B/S framework with time-dependent coefficients. Based on our formula we also derive a new semi-analytical numerical method for pricing with arbitrarily time-dependent barriers. Our approach is in the same spirit as Andricopoulos, Widdicks, Duck, and Newton (2003), but covers even wider grounds since we use the Green's function instead of the log-normal density. As a consequence we are able to model continuously observed barriers instead of discrete approximations thereof. Furthermore our formula accommodates time-dependent parameters.

Our approach turns out to be numerically stable and allows us to compute option prices for very long maturities. This numerical stability can be attributed to a set of simplifications of the general Green's function corresponding to specific rebate-boundary combinations which we provide in the Appendix. These simplifications help avoid numerical problems with singularities and transformations of infinite intervals to finite intervals.

This paper is organized as follows: Section 2 provides the Green's function result that generalizes several well-known barrier option formulae and provides the basis for our stripe method. Section 3 develops the implementation of the stripe method using Gaussian quadrature. Section 4 presents a performance analysis in which five different barrier options with several exotic features and for several maturities are priced with two different parameter scenarios. The paper ends with concluding remarks and an Appendix containing the proofs and several simplifications of the basic Green's function formula.

2 The theoretical basis

The basis for the following considerations is the B/S PDE with time-dependent coefficients:

$$\alpha(t)\, y^2\, v_{yy} + \beta(t)\, y\, v_y - r(t)\, v + v_t = 0 \qquad \text{where } y > 0 \quad \text{and} \quad 0 \le t \le \tau\,. \tag{1}$$

This formula covers derivatives written on equity driven by a GBM, as well as derivatives written on bonds that are driven by Gaussian (no state-dependent volatility) affine short rate models such as Vasicek, Ho-Lee and Hull-White (extended Vasicek). We stress that these derivatives may include time-dependent boundary conditions.

The coefficients $\alpha(t) := \frac{\sigma^2(t)}{2} > 0$, $\beta(t) := r(t) - \delta(t)$ and $r(t)$ are continuous functions of time t. The variable y represents the price of the underlying. The instantaneous interest rate is represented by $r(t)$ and $\delta(t)$ is the dividend yield. Further, let the integrals over α, β and r be denoted by

$$\tilde{\alpha}(a,b) := \int_b^a \alpha(z)\, dz, \quad \tilde{\beta}(a,b) := \int_b^a \beta(z)\, dz, \quad \tilde{r}(a,b) := \int_b^a r(z)\, dz\ . \tag{2}$$

With $0 < c_1 < c_2$ and $0 < d_1 < d_2$, the left and the right boundary r_1 and r_2 are defined by[3]

$$r_i(t) = \exp\left(\frac{\tilde{\alpha}(\tau,0)\tilde{\beta}(t,0) - \tilde{\alpha}(t,0)\tilde{\beta}(\tau,0)}{\tilde{\alpha}(\tau,0)}\right)(d_i/c_i)^{\frac{\tilde{\alpha}(t,0)}{\tilde{\alpha}(\tau,0)}}\, c_i \qquad \text{with} \quad 0 \le t \le \tau,\ \ i = 1,2\,. \tag{3}$$

At this stage the introduction of the boundaries $r_1(t)$ and $r_2(t)$ appears very arbitrary. As can be seen from the proof of the following theorem, the boundaries emerge from a trapezoidal area when transforming the Heat Equation into the Black/Scholes PDE. The set $\{(y,t) : t \in [0,\tau),\ y \in (r_1(t), r_2(t))\}$ is called the elementary area within which the solution of the PDE (1) is to be found. The corner points of this elementary area can be chosen arbitrarily, the specific boundary function is determined by formula (3). If we have $d_i = c_i$ for $i = 1,2$ and constant coefficients, then r_i are constant and equal to c_i, implying a rectangular elementary area. Let the value of $v(y,t)$ now be given on the left and the right boundary by

$$v(r_1(t),t) = \phi_1(t), \quad v(r_2(t),t) = \phi_2(t) \quad \text{for} \quad t \in [0,\tau] \tag{4}$$

[3]It is noteworthy that equation (3) generalizes the specific curved boundary type of Kunitomo and Ikeda (1992).

and at the end of the time interval $[0, \tau]$ by

$$v(y, \tau) = \varphi(y) \text{ with } y \in (d_1, d_2)\,. \tag{5}$$

Theorem 1 (Main result)**.** *The unique solution to the above boundary value problem is*

$$v(y,t) = e^{-\tilde{r}(\tau,t)} \left\{ \int_{r_1(\tau)}^{r_2(\tau)} G(x,\tau,y,t)\varphi(x)\,dx + \right. \tag{6}$$
$$\left. + \int_t^\tau e^{\tilde{r}(\tau,t')}\alpha(t')\left[r_1^2(t')G_x(r_1(t'),t',y,t)\phi_1(t') - r_2^2(t')G_x(r_2(t'),t',y,t)\phi_2(t')\right]\,dt' \right\}$$

with the basic solution

$$g(x,t',y,t) = \frac{1}{2x\sqrt{\pi\tilde{\alpha}(t',t)}} \exp\left(-\frac{\left(\ln(x/y) + \tilde{\alpha}(t',t) - \tilde{\beta}(t',t)\right)^2}{4\tilde{\alpha}(t',t)} \right) \tag{7}$$

and the Green's function

$$G(x,t',y,t) = \begin{cases} g(x,t',y,t) \sum\limits_{n=-\infty}^{\infty} (D_n - E_n) & \text{for } t < t' \\ 0 & \text{for } t \geq t' \text{ and } (x,t') \neq (y,t) \end{cases} \tag{8}$$

where D_n and E_n (both functions of x, t', y, t) are defined by

$$\begin{aligned} D_n &:= \exp(-n^2 r_2(t') \star r_2(t) - n(x \star r_2(t) - r_2(t') \star y)) \quad \text{and} \\ E_n &:= \exp(-x \star y - n^2 r_2(t') \star r_2(t) - n(x \star r_2(t) + r_2(t') \star y)) \end{aligned} \tag{9}$$

where the symbol $\star$ denotes the operation $x \star y := \frac{1}{\tilde{\alpha}(t',t)} \ln \frac{r_1(t')}{x} \ln \frac{r_1(t)}{y}$.

Proof. Appendix. □

Note that it is the special form of G that allows to model explicitly continuous observation of the right and/or left boundary. To avoid numerical problems with evaluating the general form (6) and to develop an efficient implementation it is advisable to exploit all possible simplifications that arise from vanishing boundaries (i.e. $r_1 \to 0$ or $r_2 \to \infty$) or boundary values equal to zero. We therefore provide

a table containing all of the simplifications of formula (6) for the rebate - boundary combinations that allow simplifications. In our experience it is imperative for good numerical results to make use of these simplifications whenever possible.

Since for $r_1 \to 0$ or $r_2 \to \infty$ the Green's function G reduces from an infinite series to a far simpler term, we define two simplifications of G. The function g^+ is the simplification of G for $r_2 \to \infty$, but $r_1 \not\to 0$, g^{++} corresponds to the case $r_1 \to 0$ and $r_2 \not\to \infty$:

$$g^+(x,t',y,t) = \begin{cases} g(x,t',y,t)\left(1-\exp\left(-\frac{\ln\frac{r_1(t')}{x}\ln\frac{r_1(t)}{y}}{\tilde{\alpha}(t',t)}\right)\right) & \text{for } t < t' \\ 0 & \text{for } t \geq t' \text{ and } (x,t') \neq (y,t) \end{cases}$$

$$g^{++}(x,t',y,t) = \begin{cases} g(x,t',y,t)\left(1-\exp\left(-\frac{\ln\frac{r_2(t')}{x}\ln\frac{r_2(t)}{y}}{\tilde{\alpha}(t',t)}\right)\right) & \text{for } t < t' \\ 0 & \text{for } t \geq t' \text{ and } (x,t') \neq (y,t)\,. \end{cases}$$

To obtain g^+, Theorem 2 (in the Appendix) can be applied, whereas g^{++} can be derived from Theorem 1. Table 1 gives an overview of all possible simplification cases. The corresponding formulae can be found in the Appendix.

	$r_1 \to 0,\ r_2 \not\to \infty$	$r_1 \not\to 0,\ r_2 \to \infty$	$r_1 \to 0,\ r_2 \to \infty$	else
$\phi_1 = 0$	if $\phi_2 = 0$: (A.1) if $\phi_2 \neq 0$: (A.2)	(A.3)	(A.4)	if $\phi_2 = 0$: (A.5) if $\phi_2 \neq 0$: (A.6)
$\phi_1 \neq 0$	–	(A.7)	–	if $\phi_2 = 0$: (A.8) if $\phi_2 \neq 0$: (A.9)
$\phi_1 = e^{-\tilde{r}(\tau,t)}\kappa_1$	if $\phi_2 = 0$: (A.1) if $\phi_2 \neq 0$: (A.2)	(A.10)	(A.4)	if $\phi_2 = 0$: (A.11) if $\phi_2 \neq 0$: (A.12)
$\phi_2 = e^{-\tilde{r}(\tau,t)}\kappa_2$	–	–	–	if $\phi_1 = 0$: (A.13) if $\phi_1 \neq 0$: (A.14)

Table 1: Simplifications of the main formula
Theorem 1 and Theorem 2 can be used to find simplifications of the general Green's function solution. These simplifications can be very helpful in avoiding numerical difficulties such as approximations of infinity.

The upper part of Table 1 shows the cases that can be used with the stripe method explained below. The cases in the lower part of the table can not be used in connection with the stripe method.

Illustrative Example: First, let the coefficients be constant and equal to $r \equiv 0.05$, $\delta \equiv 0.01$ and $\sigma^2 \equiv 0.09$. We consider a down-and-out call option with one barrier at $B = 8$ and strike price $K = 10$ providing a rebate of 2, payable at the expiration day, i.e. $\phi_1(t') = e^{-\tilde{r}(\tau,t')} \cdot 2$. Let the time to expiration

be half a year, $\tau = 0.5$. The boundaries here are given by $c_1 = d_1 = 8$ leading to $r_1 \equiv 8$ and by a non-existing upper boundary, $c_2 = d_2 \to \infty$. In this case simplification (A.10) can be used to price the option by

$$v(y,0) = e^{-\tilde{r}(0.5,0)} \left\{ \int_8^\infty g^+(x, 0.5, y, 0)(\max(0, x-10) - 2)\, dx + 2 \right\}. \tag{10}$$

Now we assume the instantaneous interest rate to be time dependent: $r(t) = 0.05 - 0.03\exp(-3t)$. Again setting $c_1 = d_1 = 8$ we obtain $r_1(t) = 8e^{0.01\left(2\left(e^{-1.5}-1\right)t + e^{-3t} - 1\right)}$. In this case we can only achieve a closed-form solution if the real barrier happens to be equal to r_1. Alternatively one could interpret this function as an approximation of the constant boundary at 8 which is fairly good since the relative deviation is at worst -0.14122721%. If the latter is too high, then the stripe method displayed below can be applied.

3 The stripe method and its implementation

In this section we develop an algorithm that can be used for pricing problems with boundaries that are not of the form (3). In the following we describe how to compute the value of the considered financial derivative at time $t = 0$ (valuation time) for a given spot price y^*. Thus our aim is to calculate $v(y^*, 0)$.

3.1 Simple stripe method

For piecewise differentiable arbitrary left and right boundaries r_1, r_2 we apply an iterative stripe method inspired by Hawlitschek (1989). We divide the interval $[0, \tau]$ into n intervals defined by $t_0, \ldots, t_n$, with $t_0 = \tau$, $t_n = 0$ and $t_i > t_{i+1}$. Time discretization steps t_i with $i \in \{0, 1, \ldots, n\}$ can be chosen to be equidistant. For instruments with maturities exceeding one year it is numerically advantageous to parameterize t_i with time to maturity.

Let $\hat{v}(y, t, \tau, \varphi)$ denote the value function depending on the underlying y at time t, maturity τ and final payoff function φ. When using a different instant of time s instead of τ and the function ψ instead of the original payoff function φ, the terms s and ψ are to be substituted into the formula (6) – or the simplification of choice according to Table 1 – instead of τ and φ. The formulae (A.10) to (A.14) cannot be used in connection with the stripe method due to the special form of ϕ_1 and ϕ_2 (which depend on t *and* τ).

The stripe method is an iterative algorithm starting from $t_0 = \tau$ and recursing step by step backward in time by moving from t_i to t_{i+1}.

- **Initial step:** $i = 0$

  Starting with $v(y, t_0) = \varphi(y)$, the value on the lower boundary of the first stripe, i.e. $\hat{v}(y, t_1, t_0, \varphi)$ for $y \in (r_1(t_1), r_2(t_1))$ is calculated with formula (6) or by a suitable simplification from Table 1. In practice we can only compute the value on a finite set of mesh points. This aspect will be discussed in detail below.

- After the first step we know the value function at time t_1. This function now becomes the new "payoff function" at the upper boundary of the next stripe.

- **Iterative step:** $i \to i + 1$; already known: $\psi(y) := v(y, t_i)$; wanted: $v(y, t_{i+1})$

  We find the value function at time t_{i+1} by again applying formula (6) (or a suitable simplification) to calculate $\hat{v}(y, t_{i+1}, t_i, \psi)$.

Note that in this algorithm the originally given arbitrary boundaries $r_i(t)$ with $t \in [0, \tau]$ are to be used. However, for each stripe G_i the boundaries according to (3) determined by $\alpha(t)$ and $\beta(t)$ and by the four corners $(t_{i-1}, r_1(t_{i-1}))$, $(t_{i-1}, r_2(t_{i-1}))$, $(t_i, r_1(t_i))$, $(t_i, r_2(t_i))$ differ from these. As $t_i - t_{i+1} \to 0$ not only the boundaries according to (3) converge very fast to the originally given boundaries but also the value function. See Figure 4 for an illustration of the deviation and for an impression how fast the convergence to the originally given boundaries can be.

The initial step can be carried out by applying standard adaptive numerical integration routines, because $v(y, t_0)$ is given in closed form by φ. Further, with $\psi(\cdot) := v(\cdot, t_i)$ in the iterative step we calculate $\hat{v}(y, t_{i+1}, t_i, \psi)$ by splitting the applied formula into two summands $\hat{v}_1(y, t_{i+1}, t_i, \psi)$ (the first integral) and $\hat{v}_2(y, t_{i+1}, t_i)$ (the second integral). Note that the latter one does not depend on ψ. To illustrate the procedure we take the main formula (A.9). Consider the i-th iteration. The formula can then be rewritten as the sum of $\hat{v}_1(y, t_{i+1}, t_i, \psi)$ and $\hat{v}_2(y, t_{i+1}, t_i)$ where

$$\hat{v}_1(y, t_{i+1}, t_i, \psi) = e^{-\tilde{r}(t_i, t_{i+1})} \int_{r_1(t_i)}^{r_2(t_i)} G(x, t_i, y, t_{i+1}) \nu(x, t_i)\, dx \tag{11}$$

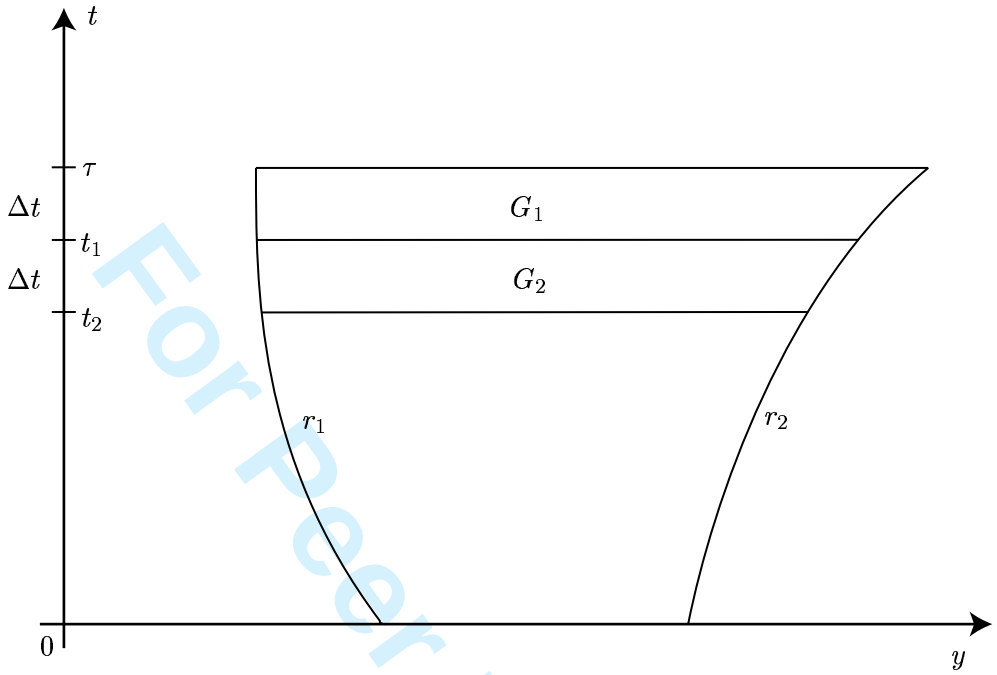

Figure 1: The stripe method
The Green's function is characterized by an end condition $\Phi(\tau)$ and two boundary conditions r_1 and r_2. When coefficients α, β and r from the PDE (1) depend on time, its solution can be approximated by solving a recursive sequence of Green's function problems of type Theorem 1.

and

$$\hat{v}_2(y, t_{i+1}, t_i) = \tag{12}$$
$$= e^{-\tilde{r}(t_i, t_{i+1})} \int_{t_{i+1}}^{t_i} e^{\tilde{r}(t_i, t')} \alpha(t') \left[r_1^2(t') G_x(r_1(t'), t', y, t) \phi_1(t') - r_2^2(t') G_x(r_2(t'), t', y, t_{i+1}) \phi_2(t') \right] dt'$$

Numerical computation of integral (12) can be done by adaptive integration. Packages are available for most platforms.[4] To compute integral (11) it is necessary to temporarily store the entire function $v(x, t_i)$ in some fashion in order to compute $\hat{v}(y, t_{i+1}, t_i, \psi)$. This is a matter of function approximation which can in principle be done with splines or Chebyshev polynomials. Numerical experiments deem the two methods unsuitable for our application.[5] Instead we achieve our results by computing values for

[4] Packages for Maple, Matlab, C/C++/Fortran/Java (with GSL, NAG, ...) or Mathematica usually provide a variety of numerical integration schemes like the Clenshaw-Curtis quadrature method, the adaptive double-exponential method, the adaptive Gaussian quadrature method, Monte Carlo integration and others.

[5] See Bates (2005) for an illustrative example in a similar context.

a discrete set of mesh points chosen according to a Gaussian quadrature rule. Non-adaptive numerical integration is then performed by simple multiplication and addition. Whenever the first integral has infinity as the upper bound it can be solved via the usual change of variable technique. As an alternative a proxy for infinity (like 5 or 10 times the strike price) also works well.

Gaussian quadrature (illustrated by Figure 2) is the preferred method for integrating smooth functions. Except for the first stripes, where the value function might exhibit problematic behavior with discontinuous or non-differentiable payoffs, value functions usually are well suited for integration with Gaussian quadrature.

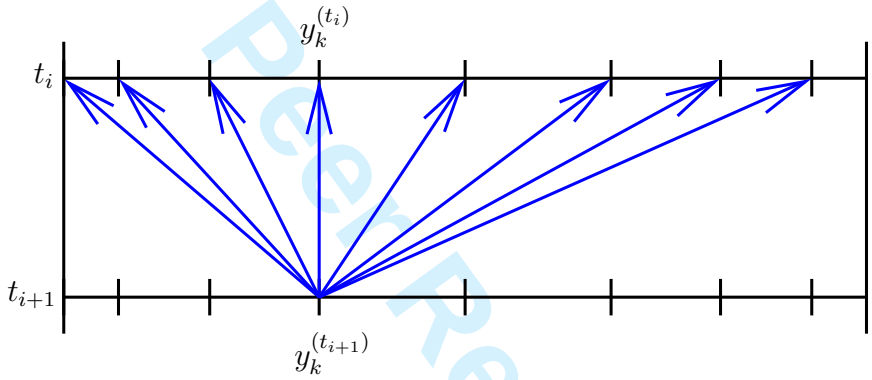

Figure 2: Gaussian quadrature with m points
The domain of the underlying asset is dissected according to an m-point Gauss rule. Most software packages include routines with $m = 10, 21, 43, 87$ since for adaptive routines the computations for the 10-point rule can be reused for the 21-rule, which in turn can be reused for the 43-rule and so on. Unfortunately the structure of the stripe method does not admit adaptive integration, but our numerical results indicate that Gaussian quadrature works well even in a non-adaptive setting like ours.

A detailed description of Gaussian quadrature can be found in Press, Teukolsky, Vetterling, and Flannery (1992). The general idea of the Gauss-Legendre routine is to approximate the integral of a function f via

$$\int_{z_1}^{z_2} f(z)dz = \sum_{j=1}^{m} w_j f(y_j)$$

where w_j and y_j denote the appropriate set of abscissas and weights respectively. The abscissas $y_j \in (z_1, z_2)$ are derived from standardized abscissas $x_j \in (-1, 1)$ by an affine transformation.

Let w_k, $k = 1, \ldots, m$ and $y_k^{(t_i)}$, $i = 0, \ldots, n-1$ denote the weights and abscissas corresponding to the m-point Gauss-Legendre rule over $(r_1(t_i)\,,\, r_2(t_i))$ respectively.

- **Initial step:** $i = 0$

Compute $\hat{v}\left(y_k^{(t_1)}, t_1, t_0, \varphi\right)$ for $k = 0, \ldots, m-1$ with standard integration routines. $(r_1(t_0)\ ,\ r_2(t_0))$.

- **Iterative step:** $i \to i+1$, $i < n-1$; already known: $\psi\left(y_k^{(t_i)}\right) := v\left(y_k^{(t_i)}, t_i\right)$ for $k = 0, \ldots, m-1$; wanted: $v\left(y_k^{(t_{i+1})}, t_{i+1}\right)$ for $k = 0, \ldots, m-1$
  Determine $\hat{v}\left(y_k^{(t_{i+1})}, t_{i+1}\right)$ for $k = 0, \ldots, m-1$ by using the formula

$$\hat{v}_1\left(y_k^{(t_{i+1})}, t_{i+1}, t_i, \psi\right) = e^{-\tilde{r}(t_i, t_{i+1})} \sum_{j=0}^{m-1} w_j G\left(y_j^{(t_i)}, t_i, y_k^{(t_{i+1})}, t_{i+1}\right) \psi\left(y_j^{(t_i)}\right) \tag{13}$$

  and by application of standard integration routines to compute $\hat{v}_2\left(y_k^{(t_{i+1})}, t_{i+1}, t_i\right)$.

- **Last step:** $n-1 \to n$; already known: $\psi\left(y_k^{(t_{n-1})}\right) := v\left(y_k^{(t_{n-1})}, t_{n-1}\right)$ for $k = 0, \ldots, m-1$; wanted: $v(y^*, t_n)$
  Determine $\hat{v}(y^*, t_n)$ by using the formula

$$\hat{v}_1(y^*, t_n, t_{n-1}, \psi) = e^{-\tilde{r}(t_{n-1}, t_n)} \sum_{j=0}^{m-1} w_j G\left(y_j^{(t_{n-1})}, t_{n-1}, y^*, t_n\right) \psi\left(y_j^{(t_{n-1})}\right) \tag{14}$$

  and by application of standard integration routines to compute $\hat{v}_2(y^*, t_n, t_{n-1})$.

Integrating over the respective partial derivative of the Green's function (instead of the Green's function itself), yields the Greeks (see Section 3.2.1 for a remark on the computation of an options's Δ when the spot underlying price is close to a barrier).

The question arises how many stripes are appropriate for the stripe method. As the number of stripes n goes to infinity the option value resulting from the stripe method converges to the exact value (see the theorems of Nagumo-Westphal for parabolic PDEs in Walter (1964, p. 158-174)).[6] In practice, convergence is obtained very fast. In our experience a number of at most 70 stripes per year is sufficient for most cases. A general scheme could be developed as follows: Determine the stripe allocation on basis of the deviation of the originally given boundaries r_1, r_2 from the boundaries resulting from formula (3). See Figure 4 for an illustration of this deviation depending on the number of stripes. It is one big advantage of our method that a very large stepwidth $t_i - t_{i+1}$ can be chosen as long as boundary deviations are small whereas methods that discretize continuous barriers can not proceed in such a way.

Section 4 suggests that one can obtain good results with as few as 10 or 40 stripes per year. In fact,

[6] The stripes are in general not anymore elementary areas with boundaries of the form (3), but differ arbitrarily little from these. If $\Delta t \to 0$ then $v(y, t)$ also fulfills PDE (1).

the precision of the Green's function method does, in general, not improve as the number of stripes increases as a consequence of cumulations of numerical errors. To make the method more precise one has to increase the number of stripes n and the number of mesh points m simultaneously since the Green's function G becomes a Dirac impulse as $\Delta t \to 0$. Numerical integration with previously fixed mesh points then becomes a delicate task. Finally, increasing n and m also has considerable performance impact.

3.2 American options

The general approach to pricing American barrier options is to determine the free boundary from the two conditions

$$v(y,t)\,\big|_{y=\rho(t)} = \varphi(y)\,\big|_{y=\rho(t)} \quad \text{(value matching)} \tag{15}$$

and

$$v_y(y,t)\,\big|_{y=\rho(t)} = \varphi'(y)\,\big|_{y=\rho(t)} \quad \text{(smooth pasting)}, \tag{16}$$

where $y > K$ for call options and $y < K$ for put options. The value matching condition is trivially satisfied if we set $\phi_i(t) = \varphi(\rho(t))$ with $i = 1$ for puts and $i = 2$ for calls. The free boundary is therefore determined by the smooth pasting condition.

For ease of exposition we will in the following restrict ourselves to American knock-out options without rebate. It is also possible to price a rebate. In this case it is necessary to incorporate the corresponding term (according to (6)) into the second integral.

3.2.1 American barrier puts

We start with the known option value at time $t_0 = \tau$, i.e. $v(y,\tau) = \varphi(y)$, and the starting point of the free boundary $\rho(\tau) = K$. The free boundary replaces r_1 while the knock-out barrier is given by r_2. The *iterative step* works from t_i to t_{i+1}. So we assume that $v(y,t_i)$ and $\rho(t_i)$ are already known.

Compute $\rho(t_{i+1})$ by numerically solving the equation

$$v_y(\rho(t_{i+1}),t_{i+1}) - \varphi'(\rho(t_{i+1})) = 0\,. \tag{17}$$

Since we have a singularity in the integrand of the second integral for $y = \rho(t_{i+1})$ we approximate

$v_y(\rho(t_{i+1}), t_{i+1})$ by:

$$\frac{1}{\epsilon}\left[v(\rho(t_{i+1})+\epsilon, t_{i+1}) - v(\rho(t_{i+1}), t_{i+1})\right] = \frac{1}{\epsilon}\left[v(\rho(t_{i+1})+\epsilon, t_{i+1}) - \varphi(\rho(t_{i+1}))\right]$$

for ϵ small enough. We have

$$\begin{aligned} v_y(\rho(t_{i+1}), t_{i+1}) \approx & -\frac{1}{\epsilon}\varphi(\rho(t_{i+1})) + \frac{e^{-\tilde{r}(t_i, t_{i+1})}}{\epsilon}\left\{\int_{\rho(t_i)}^{\infty} G(x, t_i, \rho(t_{i+1})+\epsilon, t_{i+1})\, v(x, t_i)\, dx \right. \\ & \left. + \int_{t_{i+1}}^{t_i} e^{\tilde{r}(t_i, t')}\alpha(t')\rho^2(t')G_x(\rho(t'), t', \rho(t_{i+1})+\epsilon, t_{i+1})\varphi(\rho(t'))\, dt'\right\} \end{aligned} \tag{18}$$

where $\rho(t)$ for $t \in (t_{i+1}, t_i)$ is given by (3), t_{i+1} replaces 0 and t_i replaces τ.[7] Note that for solving (17) by varying $\rho(t_{i+1})$, we need to approximate the free boundary ρ itself on the interval $[t_{i+1}, t_i]$. Boundary formula (3) is the natural candidate for this interpolation task with $c \equiv \rho(t_{i+1})$ and $d \equiv \rho(t_i)$.

After the free boundary is found it is straightforward to compute the value at the end of the stripe by:

$$v(y, t_{i+1}) = e^{-\tilde{r}(t_i, t_{i+1})}\left\{\int_{\rho(t_i)}^{\infty} G(x, t_i, y, t_{i+1})\, v(x, t_i)\, dx + \int_{t_{i+1}}^{t_i} e^{\tilde{r}(t_i, t')}\alpha(t')\rho^2(t')G_x(\rho(t'), t', y, t_{i+1})\varphi(\rho(t'))\, dt'\right\}$$

3.2.2 American barrier calls

The procedure is analogous to the one for puts with the following differences: In G the term r_1 is now the given knock-out barrier while r_2 is to be replaced by ρ. Thus the derivative $v_y(\rho(t_{i+1}), t_{i+1})$ is now

[7] Equation (18) is a numerically advantageous way to compute an option's Δ when the spot underlying price is close to the boundary due to the singularity in the exact derivative with respect to y.

approximated by:

$$\begin{aligned} v_y(\rho(t_{i+1}),t_{i+1}) &= \frac{1}{\epsilon}\left[\varphi(\rho(t_{i+1})) - v(\rho(t_{i+1})-\epsilon,t_{i+1})\right] \\ &= \frac{1}{\epsilon}\varphi(\rho(t_{i+1})) - \frac{e^{-\tilde{r}(t_i,t_{i+1})}}{\epsilon}\left\{\int_0^{\rho(t_i)} G(x,t_i,\rho(t_{i+1})-\epsilon,t_{i+1})\,v(x,t_i)\,dx\right. \\ &\quad \left. - \int_{t_{i+1}}^{t_i} e^{\tilde{r}(t_i,t')}\alpha(t')\rho^2(t')G_x(\rho(t'),t',\rho(t_{i+1})-\epsilon,t_{i+1})\varphi(\rho(t'))\,dt'\right\} \end{aligned} \tag{19}$$

After finding $\rho(t_{i+1})$ the option prices on the end of the i-th stripe can be be calculated as usual:

$$v(y,t_{i+1}) = e^{-\tilde{r}(t_i,t)}\left\{\int_0^{\rho(t_i)} G(x,t_i,y,t_{i+1})\,v(x,t_i)\,dx - \int_{t_{i+1}}^{t_i} e^{\tilde{r}(t_i,t')}\alpha(t')\rho^2(t')G_x(\rho(t'),t',y,t_{i+1})\varphi(\rho(t'))\,dt'\right\}.$$

4 Performance analysis

In order to investigate the full capabilities of the Green's function approach developed in this paper, we apply it to a number of pricing problems with time-dependent coefficients.[8] Our performance analysis contains two parameter scenarios:

- I: $r(t) = 0.05 - 0.03\exp(-3t)$; $\delta \equiv 0.01$; $\sigma^2 \equiv 0.09$
- II: $r(t) = 0.05 - 0.03\exp(-3t)$; $\delta \equiv 0$; $\sigma^2(t) = 0.08 + 0.8\exp(-4t)$

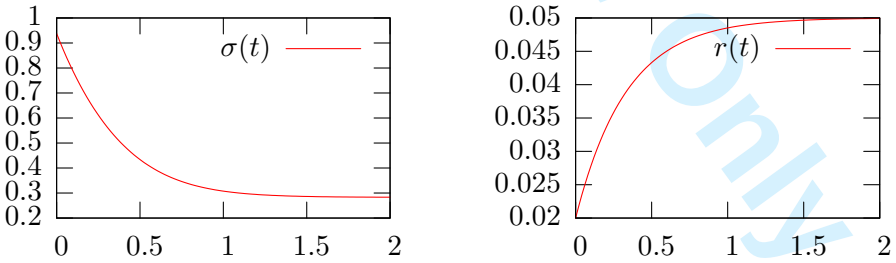

(a) Volatility Scenario II (b) Interest Rate Scenario I,II

Figure 3: Interest rates and volatility as a function of time Volatility in scenario II exceeds 90% as time t approaches zero. After approximately 1.5 years, volatility as well as interest rates become constants.

[8] Recall that European type pricing problems characterized by constant coefficients together with constant barriers or no barriers can be solved with a single numerical integration over (6).

Scenario I is relatively innocuous, whereas scenario II is more appropriate to stress test the Green's function method. Figure 3(a) displays an extreme initial volatility regime for scenario II. In both scenarios the change of r with time can be thought of as expected mean reversion of interest rates to the unconditional mean (implied by a short rate model, for example). Both, $r(t)$ and $\sigma^2(t)$ converge exponentially fast to a constant. Nevertheless up to $t = 1.5$ the functions are highly variable. Figure 4 illustrates the boundary convergence for scenario II for an originally given constant boundary at $y = 8$.

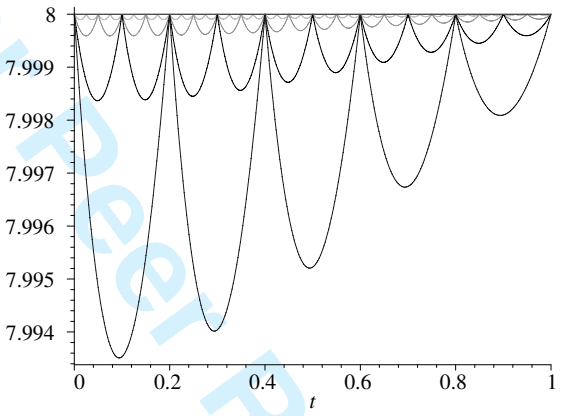

Figure 4: Convergence of boundaries approximated by the stripe method to the true boundaries Time-dependent coefficients call for an application of the stripe method to solve boundary value problems that are different from form (3). In the specific example above it can be seen that the approximation depends on time. This can be used for developing "smart stripes" that are beneficial for the computation of prices for options with long times to maturity.

For each of the scenarios and for $\tau = 0.1, 0.5, 1, 3, 5$ we examine the following options, each (except option E) with strike $K = 10$:

- A: Knock-out call with one barrier at $B = 8$ (down-and-out call)
  - A1: without rebate – formula (A.3)
  - A2: with rebate of 2, payable at the expiration day, i.e. $\phi_1(t') = e^{-\tilde{r}(\tau,t')} \cdot 2$ – formula (A.7)
- B: Knock-out put with one barrier at $B = 12$ (up-and-out put)
  - B1: without rebate – formula (A.1)
  - B2: with rebate of 2, payable at the expiration day, i.e. $\phi_2(t') = e^{-\tilde{r}(\tau,t')} \cdot 2$ – formula (A.2)
- C: Power Knock-out option, barrier at $B = 14$, exotic payoff function $\varphi(x) = (x - 10)^2$ – formula (A.1)
- D: Double-barrier call, with barriers at $B_l = 10$ and $B_u = 14$:

- D1: without rebate – formula (A.5)
- D2: with rebate = 2, payable at the expiration day, i.e. $\phi_i(t') = e^{-\tilde{r}(\tau,t')} \cdot 2$ for $i = 1, 2$ – formula (A.9)
- D3: with rebate = 2, payable at first touch of a barrier, i.e. $\phi_i(t') \equiv 2$ for $i = 1, 2$ – formula (A.9)

- E: American knock-out put with barrier $B = 6$ (no rebate) and strike $K = 5$

Options A, B, and C are valued for a present underlying spot price of $y^* = 10$, option D with $y^* = 12$ and option E with $y^* = 4$. Note that several options (A2, B2, C, D2, D3) relate to boundary value problems with discontinuities in the boundary conditions. The solution $v(y, t)$ is a continuous function, however.

A finite difference pricing framework and simulation-based pricing serve as benchmarks. We choose finite differencing for two reasons: Firstly, we need to know the "exact" value for each option and each scenario. We obtain these values by applying the Crank-Nicolson method with a very fine grid ($\Delta t, \Delta y = 0.0001$). This procedure yields very exact prices, but due to the fine mesh granularity takes too long to compete with the Green's function approach from an efficiency point of view. Therefore we additionally employ the finite difference framework with fewer mesh points in order to obtain approximation values with computation times comparable to the Green's function approach. Simulation-based pricing is chosen as an additional benchmark, since it is easy to implement and is such a widely used tool.

For the performance analysis, the Green's functions approach, the finite differencing framework, and simulation-based pricing are implemented in C++. All three approaches are parameterized with the boundary, volatility, payoff and discounting functions through the latest templating techniques. We also make use of specialized libraries. For the Green's function approach we use the GNU scientific library for standard numerical integration (second integral and first step). Our own implementation of the Gaussian quadrature as described in section 3 is done with $m = 87$ abscissas. The Crank-Nicolson routine is cast into a linear algebra problem which is solved using both the ATLAS BLAS and LAPACK routines. Random number sequences are obtained from the GNU scientific library. All computations are run on a standard Linux workstation with a single Pentium 4 processor. Our proxy for infinity is five times the strike price for finite differencing and ten times the strike price for the Green's functions approach. The proxy is lower for finite differencing, because we find the second derivative of the option price with respect to the underlying to be a boundary condition that works well at this level. For the

double barrier options D1 to D3 we reduce the series in G to the three summands for -1, 0 and 1. This is motivated by the fast convergence of the Theta series in (8) in our context.[9]

It is well known that pricing (American) barrier options by means of simulations is difficult, in particular if the underlying spot price is close to the barrier (see Gao, Huang, and Subrahmanyam, 2000). Our own experiments reveal that the time discretization steps ought to be chosen very small, in particular for the high volatility scenario. To obtain reasonable prices we have to start with as many as 20 observations per day. Since the extreme initial volatility then eases out, we linearly interpolate down to 5 observations during the first year.[10] To further improve simulation-based pricing of barrier options, in particular for our high volatility scenario, we adjust the (discretely observed) barriers by a factor $\exp\left(\pm\beta\sqrt{\int_{t_i}^{t_{i+1}}\sigma(s)^2ds}\right)$, a time-dependent version of the continuity correction proposed in Broadie, Glasserman, and Kou (1997). We cannot provide a theoretical foundation to use this method with time dependent coefficients and for correcting discretely observed barriers to continuously monitored barriers, but experiments reveil that at least with our options the method very much improves pricing accuracy. Unfortunately we experience great difficulties with double barrier option D, because we are unable to generate enough trajectories that do not touch one of the two barriers in reasonable time. As a consequence no simulation-based prices are given for this type of option. Reported MC prices are the mean of 5 simulation runs (with antithetic random variates), where each simulation is stopped as soon as 100000 trajectories have realized with no barrier events. The American barrier option E is priced with least-squares MC (LSM) from Longstaff and Schwartz (2001). Here, prices are based on 10 simulation runs with a crosssection of 10000 trajectories (with no barrier events), due to the high computer memory requirements of the LSM algorithm.

Tables 2 to 6 display the results. Each option is priced for scenario I and II. The column "exact price" in each table shows the true price, which is obtained as described above. Then for the four investigated pricing variants GF 1, GF 2, FD 1 and FD 2, we see the relative error (in percent) and the calculation time in seconds for each variant. GF 1 is short for the Green's function method with 40 stripes[11] for $\tau = 0.1, 0.5, 1$ and non-equidistant smart stripes for $\tau = 3, 5$ with time increments dt indexed by i where $dt_i = \max(a\ \exp(-b\ i), 0.02)$ with $a = 5$ and $b = 0.8$ ($\tau = 3$) and $a = 1.7$ and

[9] Theta series of the form $\sum_{n=-\infty}^{\infty} e^{-an^2+bn}$ have been a very well-known subject in mathematics since C.G.J. Jacobi (1804-1851) and have been studied in deep detail. Cf. Magnus, Oberhettinger, and Soni (1966).

[10] This fine discretization is necessary just because of the presence of barriers, since price realizations $\log y_i$ are drawn from the true transition density $\log Y_i \sim N\left(\log y_{i-1} + \int_{t_{i-1}}^{t_i}\beta(s) - \frac{\sigma^2(s)}{2}ds, \int_{t_{i-1}}^{t_i}\sigma^2(s)ds\right)$ and no discretization error arises from simulating prices.

[11] This implies an effective overall number of stripes $n = 4$ for $\tau = 0.1$, $n = 20$ for $\tau = 0.5$ and so forth.

$\tau = 0.1$			GF 1		GF 2		FD 1		FD 2		MC
		price	err. rel	time	err. rel	time	err. rel	time	err. rel	time	err. rel
A1	I	0.38466	0.0235%	0.06	0.0241%	0.00	−0.2162%	4.28	−2.3488%	0.05	0.0784%
	II	1.03465	0.0191%	0.07	0.0331%	0.00	−0.1637%	7.70	−1.7768%	0.07	0.1198%
A2	I	0.42489	0.0213%	0.14	0.0312%	0.00	−0.1963%	4.42	−2.1850%	0.05	−0.0510%
	II	1.94385	0.0219%	0.21	0.0463%	0.00	−0.0869%	7.58	−0.9318%	0.08	0.0250%
B1	I	0.37059	0.0250%	0.09	0.0249%	0.00	−0.2244%	1.19	−2.4382%	0.01	−0.0660%
	II	0.95651	0.0180%	0.15	−0.0064%	0.00	−0.1770%	2.17	−1.9162%	0.02	0.1536%
B2	I	0.47282	0.0164%	0.17	−0.0037%	0.01	−0.1767%	1.25	−1.9953%	0.01	0.1711%
	II	1.87382	−0.0057%	0.28	−0.0389%	0.00	−0.0901%	2.17	−0.9436%	0.04	0.1055%
C	I	0.89901	0.0000%	0.06	−0.0004%	0.00	−0.0004%	1.39	−0.0434%	0.01	0.4564%
	II	3.64272	−0.0014%	0.06	−0.0170%	0.00	0.0001%	2.53	0.0102%	0.03	0.2637%
D1	I	1.61736	−0.0013%	0.07	−0.0178%	0.00	0.0004%	0.40	0.0381%	0.01	—
	II	0.09198	−0.0046%	0.18	3.5698%	0.00	−0.0198%	0.73	−4.3754%	0.00	—
D2	I	1.93033	−0.0017%	0.47	−0.0194%	0.00	−0.0001%	0.42	−0.0065%	0.01	—
	II	1.98691	−0.0006%	1.21	0.0709%	0.01	0.0001%	0.73	−0.0374%	0.00	—
D3	I	1.93058	−0.0017%	0.46	−0.0194%	0.00	−0.0001%	0.40	−0.0065%	0.01	—
	II	1.99022	−0.0006%	1.19	0.0708%	0.01	0.0001%	0.74	−0.0374%	0.01	—
E	I	1.00000	0.0001%	0.56	—	—	0.0000%	0.61	0.0000%	0.00	0.3232%
	II	1.12624	−0.0003%	1.60	—	—	−0.0025%	1.05	−0.0375%	0.01	−0.2117%

Table 2: Results for instruments A, B, C, D, E for $\tau = 0.1$
Displayed are relative pricing errors and computation times for the Green's functions approach (GF), finite differences (FD) and MC simulation (MC) relative to the benchmark (finite differences according to Crank-Nicolson with $\Delta t, \Delta y = 0.0001$). Time is reported in seconds. Reported MC prices are the means of 5 simulation runs (with antithetic random variates and adaptive discretization), where each simulation is stopped as soon as 100000 trajectories have realized with no barrier events. GF prices for E are based on smart stripes, MC prices for E on the mean of 10 simulation runs with a cross section of 10000 trajectories (with no barrier events).

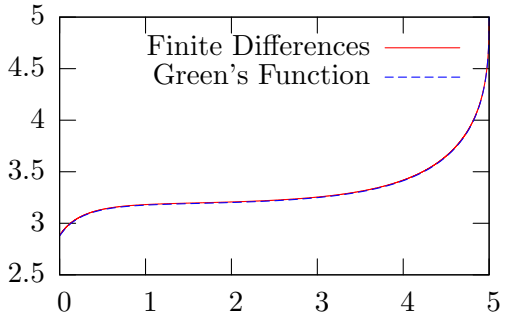

(a) Free Boundary for Scenario I (5 years)

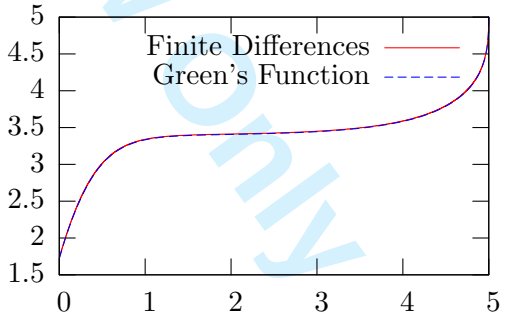

(b) Free Boundary for Scenario II (5 years)

Figure 5: Free boundaries for the American barrier option E Figures of the optimal exercise boundaries (y axis) against time (x axis) show the impact of time-dependent interest rates and volatility on the early exercise decision.

$\tau = 0.5$			GF 1		GF 2		FD 1		FD 2		MC
		price	err. rel	time	err. rel	time	err. rel	time	err. rel	time	err. rel
A1	I	0.88288	0.0039%	0.18	0.0063%	0.05	−0.0399%	16.74	−0.4419%	0.15	0.1694%
	II	1.47482	0.0127%	0.25	0.0415%	0.08	−0.0711%	27.30	−0.7868%	0.26	−0.0417%
A2	I	1.49176	0.0056%	0.62	0.0529%	0.14	−0.0870%	15.87	−0.9615%	0.15	0.1004%
	II	2.83096	0.0311%	0.88	0.0739%	0.21	−0.0862%	27.48	−0.9561%	0.27	0.0681%
B1	I	0.74227	0.0026%	0.20	−0.0019%	0.08	−0.0268%	5.55	−0.2911%	0.05	0.0521%
	II	1.20248	−0.0017%	0.32	−0.0394%	0.15	−0.0620%	7.75	−0.6823%	0.07	−0.0299%
B2	I	1.47414	−0.0842%	0.63	−0.1261%	0.17	−0.0635%	4.42	−0.7019%	0.05	−0.1068%
	II	2.45573	−0.2498%	0.94	−0.3021%	0.27	−0.0680%	7.74	−0.7521%	0.07	−0.2606%
C	I	2.66877	0.0089%	0.16	0.0039%	0.04	−0.0831%	5.38	−0.9119%	0.06	−0.1253%
	II	6.97375	0.0268%	0.25	0.0147%	0.07	−0.2537%	9.07	−2.7632%	0.08	0.1658%
D1	I	0.32485	−0.0407%	0.43	−0.0564%	0.09	0.3553%	1.53	3.9558%	0.01	—
	II	0.00021	−0.3871%	0.94	1.1397%	0.19	3.4873%	2.71	41.8526%	0.03	—
D2	I	1.94042	−0.0017%	2.74	−0.0119%	0.58	−0.0027%	1.48	−0.0303%	0.01	—
	II	1.96582	−0.0008%	5.75	0.0144%	1.21	0.0018%	2.73	0.0199%	0.03	—
D3	I	1.95801	−0.0014%	2.64	−0.0117%	0.56	−0.0052%	1.54	−0.0575%	0.02	—
	II	1.99835	−0.0005%	5.65	0.0145%	1.20	−0.0006%	2.61	−0.0071%	0.02	—
E	I	1.04107	−0.0005%	1.11	—	—	−0.0207%	2.25	−0.2016%	0.02	−0.8185%
	II	1.28218	−0.0010%	2.15	—	—	−0.0617%	3.82	−0.6174%	0.03	−0.3463%

Table 3: Results for instruments A, B, C, D, E for $\tau = 0.5$
Displayed are relative pricing errors and computation times for the Green's functions approach (GF), finite differences (FD) and MC simulation (MC) relative to the benchmark (finite differences according to Crank-Nicolson with $\Delta t, \Delta y = 0.0001$). Time is reported in seconds. Reported MC prices are the means of 5 simulation runs (with antithetic random variates and adaptive discretization), where each simulation is stopped as soon as 100000 trajectories have realized with no barrier events. GF prices for E are based on smart stripes, MC prices for E on the mean of 10 simulation runs with a cross section of 10000 trajectories (with no barrier events).

$b = 0.6$ ($\tau = 5$). GF 2 is short for the Green's function method with 10 stripes per year. For each value of τ option E is priced with smart stripes with very small time intervals near $t = \tau$, because of the the boundary's very steep slope close to maturity. For a sufficiently flat exercise boundary smart stripes are allocated as suggested in Figure 4.

The term FD 1 denotes the finite difference method with a lattice of $\Delta t, \Delta x = 0.001$, whereas FD2 corresponds to a 0.01 lattice.

$\tau = 1$			GF 1		GF 2		FD 1		FD 2		MC
		price	err. rel	time	err. rel	time	err. rel	time	err. rel	time	err. rel
A1	I	1.21921	0.0043%	0.33	0.0051%	0.08	−0.0105%	30.77	−0.1175%	0.28	0.3902%
	II	1.61163	−0.0088%	0.49	0.0300%	0.14	−0.0438%	52.87	−0.4840%	0.51	−0.1298%
A2	I	2.13632	0.0086%	1.25	0.0444%	0.29	−0.0272%	32.75	−0.3003%	0.29	−0.0328%
	II	3.01759	0.0167%	1.83	0.0693%	0.44	−0.0556%	52.49	−0.6141%	0.50	0.0147%
B1	I	0.88063	0.0000%	0.34	−0.0072%	0.12	−0.0048%	11.03	−0.0499%	0.09	0.0968%
	II	1.19017	0.0409%	0.54	−0.0430%	0.20	−0.0549%	17.98	−0.6031%	0.14	−0.2054%
B2	I	1.89054	−0.3064%	1.21	−0.3466%	0.31	−0.0169%	11.43	−0.1851%	0.09	−0.3146%
	II	2.49563	−0.7300%	1.86	−0.8081%	0.51	−0.0516%	14.93	−0.5675%	0.14	−0.7168%
C	I	3.58055	0.0058%	0.31	0.0042%	0.08	−0.0529%	10.38	−0.5796%	0.10	0.0891%
	II	7.73767	0.1909%	0.47	0.0080%	0.13	−0.1953%	17.81	−2.1244%	0.17	−0.0846%
D1	I	0.04473	−0.0401%	0.91	−0.0481%	0.21	0.3546%	2.75	3.9248%	0.02	—
	II	0.00001	−0.3849%	2.01	1.1678%	0.45	3.4870%	4.79	41.6367%	0.05	—
D2	I	1.91723	−0.0020%	5.74	−0.0105%	1.32	0.0012%	2.83	0.0134%	0.03	—
	II	1.92063	−0.0008%	12.19	0.0144%	2.84	0.0018%	4.81	0.0202%	0.05	—
D3	I	1.97656	−0.0016%	5.56	−0.0102%	1.27	−0.0019%	2.75	−0.0207%	0.03	—
	II	1.99836	−0.0005%	11.99	0.0145%	2.79	−0.0006%	4.80	−0.0068%	0.05	—
E	I	1.09321	−0.0005%	1.52	—	—	−0.0178%	4.23	−0.1773%	0.05	−1.5451%
	II	1.30687	−0.0009%	3.23	—	—	−0.0508%	7.20	−0.5074%	0.08	−1.2328%

Table 4: Results for instruments A, B, C, D, E for $\tau = 1$
Displayed are relative pricing errors and computation times for the Green's functions approach (GF), finite differences (FD) and MC simulation (MC) relative to the benchmark (finite differences according to Crank-Nicolson with $\Delta t, \Delta y = 0.0001$). Time is reported in seconds. Reported MC prices are the means of 5 simulation runs (with antithetic random variates and adaptive discretization), where each simulation is stopped as soon as 100000 trajectories have realized with no barrier events. GF prices for E are based on smart stripes, MC prices for E on the mean of 10 simulation runs with a cross section of 10000 trajectories (with no barrier events).

Tables 2 to 6 suggest the Green's function method to be a competitive alternative to finite differencing. For the options and scenarios considered in our test case, both finite differences, and Green's functions appear to be superior to MC simulation. Time consumption for MC simulation is not reported in the tables, but runtimes are considerably slower than for FD and GF (from about 100 s for $\tau = 0.1$ up to more than 3600 s for $\tau = 5$, because so few trajectories do not trigger barrier events). In particular we make the following observations:

- The number of stripes needed for reasonable results depends on the time variation behavior of the coefficients. Scenario I can be regarded as "smoother" than scenario II, in which it is harder to achieve an error close to zero. One can see that the stripe method with 10 stripes per year is sufficiently precise in nearly all of the scenario I cases. The worst observed deviation is −0.3466% for $\tau = 1$ with option B2. For scenario II GF 1 results are very precise, but 10 stripes (GF 2) appear insufficient. The worst case here is again option B2 with $\tau = 1$, with a relative error of −0.73%. Note that this option poses an extreme difficulty for Green's functions, since the rebate

$\tau = 3$			GF 1		GF 2		FD 1		FD 2		MC
		price	err. rel	time	err. rel	time	err. rel	time	err. rel	time	err. rel
A1	I	1.80051	0.0054%	0.20	−0.0035%	0.22	0.0044%	87.56	0.0472%	0.83	0.0632%
	II	1.91959	−0.1744%	0.32	−0.7614%	0.36	−0.0026%	149.16	−0.0255%	1.44	−0.0539%
A2	I	3.01651	−0.7017%	0.82	−0.6648%	0.84	−0.0033%	92.35	−0.0365%	0.87	−0.8817%
	II	3.36445	−2.2841%	1.14	−2.5581%	1.30	−0.0268%	146.24	−0.2910%	1.41	−2.3363%
B1	I	0.90527	−0.0078%	0.22	−0.0269%	0.25	−0.0012%	24.42	−0.0113%	0.24	0.1038%
	II	1.03202	−0.0108%	0.38	−0.1538%	0.41	−0.0484%	41.83	−0.5300%	0.42	0.0349%
B2	I	2.16261	−1.2961%	0.76	−1.3678%	0.86	−0.0042%	24.37	−0.0444%	0.23	−1.3158%
	II	2.37804	−3.0496%	1.21	−3.1866%	1.36	−0.0391%	40.89	−0.4256%	0.41	−3.0262%
C	I	5.75269	−0.0011%	0.17	0.0009%	0.21	−0.0212%	28.60	−0.2314%	0.27	0.2415%
	II	8.01352	0.0088%	0.30	−0.0376%	0.35	−0.1303%	59.75	−1.4151%	0.59	0.1547%
D1	I	0.00002	−0.0408%	2.74	−0.0664%	0.68	0.3536%	8.32	3.8203%	0.08	—
	II	0.00000	−0.3809%	5.99	121.3214%	1.48	3.4862%	14.02	41.5329%	0.14	—
D2	I	1.73872	−0.0008%	3.66	−0.0281%	4.08	0.0018%	7.88	0.0203%	0.07	—
	II	1.73872	−0.0009%	7.92	0.2002%	8.93	0.0018%	14.00	0.0203%	0.15	—
D3	I	1.97935	−0.0006%	3.53	−0.0278%	3.94	−0.0014%	8.26	−0.0151%	0.08	—
	II	1.99836	−0.0006%	7.81	0.1969%	8.73	−0.0006%	13.86	−0.0068%	0.14	—
E	I	1.15333	−0.0011%	2.62	—	—	−0.0119%	12.14	−0.1164%	0.12	−5.7455%
	II	1.32105	−0.0037%	3.56	—	—	−0.0446%	20.86	−0.4482%	0.20	−5.3367%

Table 5: Results for instruments A, B, C, D, E for $\tau = 3$
Displayed are relative pricing errors and computation times for the Green's functions approach (GF), finite differences (FD) and MC simulation (MC) i relative to the benchmark (finite differences according to Crank-Nicolson with $\Delta t, \Delta y = 0.0001$). Time is reported in seconds. GF 1 prices are based on smart stripes, GF 2 prices on 10 stripes per year. Reported MC prices are the means of 5 simulation runs (with antithetic random variates and adaptive discretization), where each simulation is stopped as soon as 100000 trajectories have realized with no barrier events. GF prices for E are based on smart stripes, MC prices for E on the mean of 10 simulation runs with a cross section of 10000 trajectories (with no barrier events).

puts a high value into a region where the option actually is far out of the money thus causing a huge discontinuity between the boundary and the end condition of the PDE problem.

- There are some cases where the Green's function approach is slower than FD, in particular with options D2 and D3 where the boundaries lie relatively close together, thus making the FD algorithms fast, and where the second integral does not simplify at all, which makes the GF method slower.
- Looking at the results for option A1 (scenario I) for $\tau = 1$ we see that GF 1 is over 93 times faster than FD 1, but is 2.4 times as accurate at the same time. Compared to FD 2 it takes about the same time but is 27 times as accurate. The values are similar for scenario II. Considering option C for $\tau = 0.5$ reveals a calculation time of GF 2 that is 134 times shorter than the one of FD 1, but the precision is 21fold.
- MC pricing accuracy can not compete with GF or FD for our test cases; MC is also much slower.

$\tau = 5$			GF 1		GF 2		FD 1		FD 2		MC
		price	err. rel	time	err. rel	time	err. rel	time	err. rel	time	err. rel
A1	I	2.05123	−0.0028%	0.34	−1.1553%	0.37	0.0059%	152.48	0.0663%	1.44	−0.1499%
	II	2.12679	−0.5184%	0.57	−5.3468%	0.61	0.0141%	246.81	0.1547%	2.38	0.0504%
A2	I	3.27934	−1.1113%	1.39	−1.8052%	1.43	−0.0012%	144.97	−0.0122%	1.38	−1.0106%
	II	3.53455	−3.7632%	2.05	−6.6417%	2.24	−0.0167%	247.40	−0.1774%	2.38	−3.5571%
B1	I	0.81422	−0.0013%	0.36	−0.0085%	0.36	−0.0036%	41.55	−0.0359%	0.41	0.0595%
	II	0.88940	0.0385%	0.64	−0.0280%	0.63	−0.0485%	69.10	−0.5284%	0.68	−0.0072%
B2	I	2.07016	−2.2506%	1.33	−2.2820%	1.46	−0.0063%	39.97	−0.0681%	0.39	−2.2545%
	II	2.22074	−5.3047%	2.10	−5.3746%	2.31	−0.0405%	69.35	−0.4408%	0.68	−5.3660%
C	I	6.49914	0.0007%	0.31	0.0006%	0.35	−0.0128%	48.77	−0.1388%	0.48	−0.2396%
	II	7.71937	0.1100%	0.53	0.0242%	0.60	−0.1029%	85.44	−1.1151%	0.84	0.0846%
D1	I	0.00000	−0.1241%	1.05	−0.0457%	1.20	0.3526%	13.06	3.7160%	0.13	—
	II	0.00000	5.75269%	2.33	1.1853%	2.62	3.4837%	24.35	41.1712%	0.23	—
D2	I	1.57326	−0.0012%	6.44	−0.0105%	7.13	0.0018%	13.77	0.0203%	0.16	—
	II	1.57326	−0.0007%	14.08	0.0144%	15.62	0.0018%	24.33	0.0203%	0.23	—
D3	I	1.97936	−0.0009%	6.25	−0.0102%	6.90	−0.0014%	14.41	−0.0151%	0.14	—
	II	1.99836	−0.0004%	13.86	0.0145%	15.37	−0.0006%	24.53	−0.0068%	0.22	—
E	I	1.15902	−0.0020%	3.33	—	—	−0.0112%	20.09	−0.1105%	0.20	−11.8835%
	II	1.32211	−0.0050%	4.52	—	—	−0.0447%	34.37	−0.4444%	0.36	−11.8580%

Table 6: Results for instruments A, B, C, D, E for $\tau = 5$
Displayed are relative pricing errors and computation times for the Green's functions approach (GF), finite differences (FD) and MC simulation (MC) relative to the benchmark (finite differences according to Crank-Nicolson with $\Delta t, \Delta y = 0.0001$). Time is reported in seconds. GF 1 prices are based on smart stripes, GF 2 prices on 10 stripes per year. Reported MC prices are the means of 5 simulation runs (with antithetic random variates and adaptive discretization), where each simulation is stopped as soon as 100000 trajectories have realized with no barrier events. GF prices for E are based on smart stripes, MC prices for E on the mean of 10 simulation runs with a cross section of 10000 trajectories (with no barrier events).

- The Green's function method performs very well for American barrier options, in particular for longer maturities.[12]

Figures 5(a) and 5(b) show that the free boundaries computed by finite differences are almost indistinguishable from the free boundaries computed with the Green's function pricing algorithm from 3.2.1.

For all above barrier options, the barriers were constant and application of the stripe method was only necessary due to non-constant coefficients. However, the stripe method can be applied in the same manner to problems with curved barriers. This is an advantage of the stripe method in contrast to finite differencing or lattice methods where it is difficult to handle curved barriers that do not agree with the discrete nature of mesh points. As an example we consider a variation of a D type double-barrier call (with $K = 12$). Let τ be $\tau = 1$ and let the curved barriers be at $r_1(t) = 4 + 6^t$, $r_2(t) = 20 - 6^t$,

[12]Finite differencing would have taken considerably longer for the American barrier option if the barrier had been higher, while there would have been no performance impact for Green's functions runtimes.

where a rebate of 2 is triggered, payable at the expiration day: $\phi_i(t') = e^{-\tilde{r}(\tau,t')} \cdot 2$ for $i = 1, 2$. It does not take longer than pricing option D2 from above to find the price with 40 stripes for scenario I (price: 1.858933222960536) and for scenario II (price: 1.887128873096263) and no modifications of the algorithm are necessary.

5 Conclusion

The Green's function approach presented in this paper is a new technique to solve option pricing problems within the Black/Scholes PDE framework when coefficients depend on time. We show that several cases even admit a closed-form solution. When there is no closed-form solution, a recursive numerical method (*stripe method*) can be applied which makes use of the structure of the closed-form solution. The stripe method is easily implemented and numerically reliable. Furthermore it can be used to price American options by iteratively finding the optimal exercise boundary. Empirical results obtained by following our implementational guidelines indicate that the Green's function approach is very suitable for the pricing of options with difficult features such as:

1. Time-dependent coefficients of the underlying process
2. Time-dependent, continuously observed barriers
3. Spot underlying prices close to the barriers
4. Long maturities
5. Early exercise rights

Clearly our approach is also capable of pricing simpler financial products, such as European plain vanilla options. For our test cases we find that the Green's function method developed in this paper exhibits results that are comparable and in most cases better than finite differencing from a time consumption – pricing accuracy point of view; both finite differencing and Green's functions are found to be superior to Monte Carlo simulation.

Interesting future research topics arise naturally with our approach. The extension of the Green's functions approach to state-dependent coefficients seems to be in reach. This would enable the researcher to shed new light on the literature on volatility smiles and skews. Also, bond options with barriers could be priced with short rate models from the square-root family such as CIR or Hull/White.

References

Andricopoulos, A., M. Widdicks, P. Duck, and D. Newton, 2003, "Universal Option Pricing Using Quadrature," *Journal of Financial Economics*, 67, 447–471.

Bates, D., 2005, "Maximum Likelihood Estimation of Latent Affine Processes," *Review of Financial Studies*, forthcoming.

Beaglehole, D., and M. Tenney, 1992, "A Nonlinear Equilibrium Model of the Term Structure of Interest Rates: Corrections and Additions," *Journal of Financial Economics*, 35, 345–354.

Broadie, M., P. Glasserman, and S. Kou, 1997, "A Continuity Correction For Discrete Barrier Options," *Mathematical Finance*, 7, 325–348.

Büttler, H.-J., and J. Waldvogel, 1996, "Pricing Callable Bonds by Means of Green's Function," *Mathematical Finance*, 6, 53–88.

Duffie, D., 2001, *Dynamic Asset Pricing*, Princeton University Press, Princeton and Oxford.

Gao, B., J. Huang, and M. Subrahmanyam, 2000, "The valuation of American barrier options using the decomposition technique," *Journal of Economic Dynamics & Control*, 24, 1783–1827.

Haug, E., 1997, *The Complete Guide to Option Pricing Formulas*, McGraw-Hill, New York et al.

Hawlitschek, K., 1960, "Greensche Funktionen für Randwertaufgaben partieller Differentialgleichungen vom parabolischen Typ," *Mathematische Annalen*, 160, 65–75.

Hawlitschek, K., 1989, "Approximation Greenscher Funktionen bei Parabolischen Differenzialgleichungen," *Journal of Applied Mathematics and Physics (ZAMP)*, 40, 912–919.

Hui, C., C. Lo, and P. Yuen, 2000, "Comment on 'Pricing double barrier options using Laplace transforms' by Antoon Pelsser," *Finance and Stochastics*, 4, 104–107.

John, F., 1986, *Partial Differential Equations*, Springer, New York.

Kunitomo, N., and M. Ikeda, 1992, "Pricing Options with Curved Boundaries," *Mathematical Finance*, 2, 275–298.

Lo, C. F., H. C. Lee, and C. H. Hui, 2003, "A Simple Approach for Pricing Barrier Options with Time-Dependent Parameters," *Quantitative Finance*, 3, 98–107.

Longstaff, F. A., and E. S. Schwartz, 2001, "Valuing American Options by Simluation: A simple Least-Squares Approach," *Review of Financial Studies*, 14, 113–147.

Magnus, W., F. Oberhettinger, and R. Soni, 1966, *Formulas and Theorems for the Special Functions of Mathematical Physics*, Springer, Berlin.

Mallier, R., and A. Deakin, 2003, "A Green's Function for Convertible Bonds using the Vasicek model," *Journal of Applied Mathematics*, 2, 219–232.

Press, W., S. Teukolsky, W. Vetterling, and B. Flannery, 1992, *Numerical Recipes in C*, Cambridge University Press, New York.

Roberts, G., and C. Shortland, 1997, "Pricing Barrier Options with Time-Dependent Coefficients," *Mathematical Finance*, 7, 83–93.

Staunton, M., 2005, *The Best of Wilmott 2* . chap. Efficient estimates for valuing American options, Wiley.

Walter, W., 1964, *Differential- und Integral-Ungleichungen*, Springer, Berlin.

Wilmott, P., 2000, *Paul Wilmott on Quantitative Finance:* . , vol. I, Wiley, Chichester et al.

Zhang, P., 2001, *Exotic Options - A Guide to Second Generation Options*, World Scientific Publishing, Singapore, 2 edn.

Appendix

Proof of Theorem 1

Proof. We start with the Green's function for the so-called first boundary value problem of the Heat Equation. In a second step we transform the variables and end up with the Green's function belonging to (1).

I. (Green's function of the Heat Equation) We consider the Green's function $\Gamma_0(X, T', Y, T)$ of the Heat Equation

$$\Gamma_{0XX} - \Gamma_{0T'} = 0$$

respectively the adjoint equation

$$\Gamma_{0YY} + \Gamma_{0T} = 0\,,$$

with boundary conditions

$$\Gamma_0 = 0 \quad \text{for} \quad Y = R_i(T) \quad i = 1,2 \quad \text{or} \quad X = R_i(T')\,, \quad i = 1,2$$

where the left boundary R_1 and the right boundary R_2 are

$$R_i(T) = m_i T + o_i \quad \text{with } i = 1,2\,, \tag{20}$$

i.e. we have a trapezoid-like elementary area. Hawlitschek (1960) gives the unique representation of the Green's function Γ_0 by:

$$\Gamma_0(X, T', Y, T) = \begin{cases} \frac{1}{2\sqrt{\pi(T'-T)}} \exp\left(-\frac{(X-Y)^2}{4(T'-T)}\right) \sum_{n=-\infty}^{\infty} \left(\tilde{D}_n - \tilde{E}_n\right) & \text{for } T < T' \\ 0 & \text{for } T \geq T' \text{ and } (X,T') \neq (Y,T) \end{cases} \tag{21}$$

with the abbreviations

$$\tilde{D}_n := \exp(-n^2 R_2 \odot R_2 - n(X \odot R_2 - R_2 \odot Y)) \quad \text{and} \quad \tilde{E}_n := \exp(-X \odot Y - n^2 R_2 \odot R_2 - n(X \odot R_2 + R_2 \odot Y))\,.$$

and

$$X \odot Y := \frac{1}{T'-T}\left(R_1(T')-X\right)\left(R_1(T)-Y\right), \quad X \odot R_2 := \frac{1}{T'-T}\left(R_1(T')-X\right)\left(R_1(T)-R_2(T)\right),$$

$$R_2 \odot Y := \frac{1}{T'-T}\left(R_1(T')-R_2(T')\right)\left(R_1(T)-Y\right), \quad R_2 \odot R_2 := \frac{1}{T'-T}\left(R_1(T')-R_2(T')\right)\left(R_1(T)-R_2(T)\right). \tag{22}$$

II. (Transformation) To achieve the Green's function of the more general PDE

$$\alpha(t)\, y^2\, u_{yy} + \beta(t)\, y\, u_y + u_t = 0\,, \tag{23}$$

we apply the following transformation (with $x, y > 0$)

$$X = \ln x + \tilde{\alpha}(t',0) - \tilde{\beta}(t',0), \quad Y = \ln y + \tilde{\alpha}(t,0) - \tilde{\beta}(t,0), \quad T' = \tilde{\alpha}(t',0), \quad T = \tilde{\alpha}(t,0)\,. \tag{24}$$

We now define

$$\Gamma(x,t',y,t) := \frac{1}{x}\Gamma_0(X,T',Y,T) = \frac{1}{x}\Gamma_0(\ln x + \tilde{\alpha}(t',0) - \tilde{\beta}(t',0), \tilde{\alpha}(t',0), \ln y + \tilde{\alpha}(t,0) - \tilde{\beta}(t,0), \tilde{\alpha}(t,0))\,. \tag{25}$$

Transformation (24) makes it necessary to substitute

$$T'-T \quad \text{by} \quad \tilde{\alpha}(t',t) \qquad \text{and} \qquad -\frac{(X-Y)^2}{4(T'-T)} \quad \text{by} \quad -\frac{\left(\ln(x/y) + \tilde{\alpha}(t',t) - \tilde{\beta}(t',t)\right)^2}{4\tilde{\alpha}(t',t)}$$

in equation (21). Applying (24) to the boundaries $X = R_i(T)$ and $Y = R_i(T')$ yields new boundaries characterized by x resp. y equal to

$$\exp\left(m_i\tilde{\alpha}(t,0) - \tilde{\alpha}(t,0) + \tilde{\beta}(t,0) + o_i\right) \quad \text{for } i = 1,2\,.$$

If we choose o_i and m_i as

$$o_i := \ln c_i \quad \text{and} \quad m_i := 1 + \frac{\ln(d_i/c_i) - \tilde{\beta}(\tau,0)}{\tilde{\alpha}(\tau,0)} \quad \text{for } i = 1,2\,,$$

the left and right boundary are equal to (3). Now, a little algebra shows that applying the transformation

(24) to (22) leads to substituting

$$X \odot Y \quad \text{by} \quad x \star y, \quad X \odot R_2 \quad \text{by} \quad x \star r_2, \quad R_2 \odot Y \quad \text{by} \quad r_2 \star y, \quad \text{and} \quad R_2 \odot R_2 \quad \text{by} \quad r_2 \star r_2$$

in $\tilde{D}_n$ and $\tilde{E}_n$, yielding D_n and E_n. Equation (25) defines the Green's function of the PDE with boundary conditions $\Gamma = 0$ for $y = r_i(t)$, $i = 1, 2$, or $x = r_i(t')$, $i = 1, 2$.

III. (Constructing the unique solution) With the Green's function Γ according to (25) we define

$$u(y,t) := \int_{r_1(\tau)}^{r_2(\tau)} \Gamma(x,\tau,y,t)\varphi(x)\,dx + \int_t^\tau \alpha(t')\left[r_1^2(t')\Gamma_x(r_1(t'),t',y,t)\phi_1(t') - r_2^2(t')\Gamma_x(r_2(t'),t',y,t)\phi_2(t')\right]\,dt'\,.$$

The function $u(y,t)$ inherits the property of satisfying PDE (23) from Γ. The boundary conditions (4) and (5) for u instead of v hold due to basic Green's function theory.[13] Next, we define $v(y,t)$ as in (6).

By the use of the product rule we see that $v(y,t)$ satisfies PDE (1). The boundary conditions (4) are satisfied, because of

$$e^{-\tilde{r}(\tau,t)} \cdot e^{\tilde{r}(\tau,t)}\phi_i(t) = \phi_i(t) \text{ for } i = 1, 2\,.$$

The end condition (5) holds because of $e^{-\tilde{r}(\tau,\tau)} = 1$. Thus, $v(y,t)$ is the unique solution of the boundary value problem (1) with boundary conditions (4) and (5) and the claim is proven.[14] □

[13] (Cf. Hawlitschek, 1960, p. 74)

[14] For a more detailled argumentation in the sense of partial differential equation theory, see Hawlitschek (1960).

Theorem 2 (Alternative representation of the unique Green's function)**.** *The Green's function can also be expressed by*

$$G(x,t',y,t) = \begin{cases} g(x,t',y,t) \sum\limits_{n=-\infty}^{\infty} \left(\check{D}_n - \check{E}_n\right) & \text{for } t < t' \\ 0 & \text{for } t \geq t' \text{ and } (x,t') \neq (y,t) \end{cases} \tag{26}$$

where $\check{D}_n$ *and* $\check{E}_n$ *(both functions of* x,t',y,t*) are defined by*

$$\begin{aligned} \check{D}_n &:= \exp(-n^2 r_1(t') \check{\star} r_1(t) - n(x \check{\star} r_1(t) - r_1(t') \check{\star} y)) \quad \text{and} \\ \check{E}_n &:= \exp(-x \check{\star} y - n^2 r_1(t') \check{\star} r_1(t) - n(x \check{\star} r_1(t) + r_1(t') \check{\star} y)) \end{aligned} \tag{27}$$

where the symbol $\check{\star}$ *denotes the operation* $x \check{\star} y := \frac{1}{\tilde{\alpha}(t',t)} \ln \frac{r_2(t')}{x} \ln \frac{r_2(t)}{y}$.

Proof. The proof can be done completely analogous to the proof of Theorem 1 by exchanging r_1 and r_2. This is possible because the property $r_2(t) > r_1(t)$ is not used in the proof. The claim follows by the uniqueness of the Green's function. □

Simplifications

$$e^{-\tilde{r}(\tau,t)} \int_0^{r_2(\tau)} g^{++}(x,\tau,y,t)\varphi(x)\,dx \tag{A.1}$$

$$e^{-\tilde{r}(\tau,t)} \left\{ \int_0^{r_2(\tau)} g^{++}(x,\tau,y,t)\varphi(x)\,dx - \int_t^{\tau} e^{\tilde{r}(\tau,t')} \alpha(t') r_2^2(t') g_x^{++}(r_2(t'),t',y,t)\phi_2(t')\,dt' \right\} \tag{A.2}$$

$$e^{-\tilde{r}(\tau,t)} \int_{r_1(\tau)}^{\infty} g^{+}(x,\tau,y,t)\varphi(x)\,dx \tag{A.3}$$

$$e^{-\tilde{r}(\tau,t)} \int_0^{\infty} g(x,\tau,y,t)\varphi(x)\,dx \tag{A.4}$$

$$e^{-\tilde{r}(\tau,t)} \int_{r_1(\tau)}^{r_2(\tau)} G(x,\tau,y,t)\varphi(x)\,dx \tag{A.5}$$

$$e^{-\tilde{r}(\tau,t)} \left\{ \int_{r_1(\tau)}^{r_2(\tau)} G(x,\tau,y,t)\varphi(x)\,dx - \int_t^{\tau} e^{\tilde{r}(\tau,t')}\alpha(t')r_2^2(t')G_x(r_2(t'),t',y,t)\phi_2(t')\,dt' \right\} \tag{A.6}$$

$$e^{-\tilde{r}(\tau,t)} \left\{ \int_{r_1(\tau)}^{\infty} g^+(x,\tau,y,t)\varphi(x)\,dx + \int_t^{\tau} e^{\tilde{r}(\tau,t')}\alpha(t')r_1^2(t')g_x^+(r_1(t'),t',y,t)\phi_1(t')\,dt' \right\} \tag{A.7}$$

$$e^{-\tilde{r}(\tau,t)} \left\{ \int_{r_1(\tau)}^{r_2(\tau)} G(x,\tau,y,t)\varphi(x)\,dx + \int_t^{\tau} e^{\tilde{r}(\tau,t')}\alpha(t')r_1^2(t')G_x(r_1(t'),t',y,t)\phi_1(t')\,dt' \right\} \tag{A.8}$$

$$\begin{aligned} e^{-\tilde{r}(\tau,t)} \Bigg\{ & \int_{r_1(\tau)}^{r_2(\tau)} G(x,\tau,y,t)\varphi(x)\,dx + \\ & + \int_t^{\tau} e^{\tilde{r}(\tau,t')}\alpha(t') \left[r_1^2(t')G_x(r_1(t'),t',y,t)\phi_1(t') - r_2^2(t')G_x(r_2(t'),t',y,t)\phi_2(t') \right] dt' \Bigg\} \end{aligned} \tag{A.9}$$

$$e^{-\tilde{r}(\tau,t)} \left\{ \int_{r_1(\tau)}^{\infty} g^+(x,\tau,y,t)(\varphi(x)-\kappa_1)\,dx + \kappa_1 \right\} \tag{A.10}$$

$$e^{-\tilde{r}(\tau,t)}\left\{\int_{r_1(\tau)}^{r_2(\tau)} G(x,\tau,y,t)\varphi(x)\,dx + \int_t^\tau \alpha(t')r_1^2(t')G_x(r_1(t'),t',y,t)\kappa_1\,dt'\right\} \tag{A.11}$$

$$e^{-\tilde{r}(\tau,t)}\left\{\int_{r_1(\tau)}^{r_2(\tau)} G(x,\tau,y,t)[\varphi(x)-\kappa_1]\,dx - \right. \tag{A.12}$$
$$\left. -\int_t^\tau \alpha(t')r_2^2(t')G_x(r_2(t'),t',y,t)[e^{\tilde{r}(\tau,t')}\phi_2(t')-\kappa_1]\,dt' + \kappa_1\right\}$$

$$e^{-\tilde{r}(\tau,t)}\left\{\int_{r_1(\tau)}^{r_2(\tau)} G(x,\tau,y,t)\varphi(x)\,dx - \int_t^\tau \alpha(t')r_2^2(t')G_x(r_2(t'),t',y,t)\kappa_2\,dt'\right\} \tag{A.13}$$

$$e^{-\tilde{r}(\tau,t)}\left\{\int_{r_1(\tau)}^{r_2(\tau)} G(x,\tau,y,t)[\varphi(x)-\kappa_2]\,dx - \right. \tag{A.14}$$
$$\left. -\int_t^\tau \alpha(t')r_1^2(t')G_x(r_1(t'),t',y,t)[e^{\tilde{r}(\tau,t')}\phi_1(t')-\kappa_2]\,dt' + \kappa_2\right\}$$